

An Integrated Heater Equalizer for Lithium-Ion Batteries of Electric Vehicles

Yunlong Shang , *Member, IEEE*, Chong Zhu , *Member, IEEE*, Yuhong Fu,
and Chunting Chris Mi , *Fellow, IEEE*

Abstract—In this paper, an automotive onboard heater equalizer is proposed to heat low-temperature batteries and balance cell voltages without the requirement of external power supplies. The proposed integrated topology only needs one MOSFET for one cell, resulting in a compact size and low cost, which can be easily applied to electric vehicles. In particular, all MOSFETs are driven by one high-frequency pulsewidth modulation signal and the batteries can be heated internally by the ohmic and electrochemical losses and warmed externally by the switching and conduction losses of MOSFETs, leading to a high heating speed and efficiency. Further, a thermoelectric model for the internal and external combined heating is developed to provide guidance for the optimized design of the proposed heater. In addition, the proposed topology can realize passive balancing of series-connected battery strings at a higher switching frequency and a smaller duty cycle. Experimental results show that the proposed heater, by generating a periodic ramped discharge current with an rms value of 1.8 C at a switching frequency of 150 kHz, can heat the lithium-ion batteries from -20 to 0 °C within 1.9 min, consuming about 5% of the cell energy.

Index Terms—Battery heaters, battery management systems, electric vehicles (EVs), passive equalizers, thermoelectric models.

I. INTRODUCTION

AT LOW temperatures, the driving range of electric vehicles (EVs) will drop tremendously due to the drastic increase of the internal resistances of lithium-ion battery strings, causing severe loss of usable energy and power [1]–[5]. For example, the average battery range of EVs dropped 57% at -6.7 °C compared with that at 23.9 °C [6]. In particular, battery usage in a cold climate also accelerates battery degradation [7]–[9]. Therefore, in cold climates, the onboard lithium-ion batteries of EVs should be preheated before driving.

In addition, lithium-ion battery cells are usually connected in series and parallel to meet the load demands [10], [11]. For example, there are 7104 lithium-ion cells in the battery pack of

Tesla Model S [12]. Nevertheless, the inconsistencies of the cell voltages and capacities caused by the inevitable slight differences in battery cells would be enlarged on repeated charging and discharging [13]. In order to prevent lithium plating and battery damage, cell voltages should be limited within a safe range, which results in a tremendous reduction in the usable energy and lifetime of battery packs [10], [14]. For example, the available capacity and cycle life of an eight-cell series-connected battery string without balancing are lower than 86% and 33% of the cells with balancing, respectively [10], [11]. Therefore, battery balancing is necessary to ensure the good consistency of the cell voltages to maximize the usable energy and lifetime of series-connected battery packs.

In summary, battery operation at low temperatures and the imbalance in cell voltages will lead to a serious decrease in the driving range of EVs and battery lifetime. Therefore, preheating cold lithium-ion batteries before driving and balancing inconsistent cell voltages have become imperious demands to improve the performances of EVs.

According to the survey, battery-heating methods can be divided into external and internal heating solutions [15]–[19]. External heating solutions usually use external heating devices, e.g., electric resistance wires, to first heat air or liquid and then deliver the warm air or liquid to batteries [17]–[19]. Therefore, external heating solutions have the obvious disadvantages of bulky size, high cost, bad consistency, and heat dissipation to the environment, resulting in an unsatisfactory heating performance. In particular, due to the requirement of external power sources, the external heating methods cannot be directly applied to EVs.

In contrast, the internal heating methods can warm batteries using the heat generated by the ohmic resistance and the electrochemical reaction rather than using external heaters, eliminating the long paths of heat conduction and reducing the heat radiation to the environment [18], [19]. Therefore, the internal heating solutions have the potential to provide a faster speed and higher efficiency for warming batteries. Further, the internal heating can be classified into the direct-current (dc) and alternating-current (ac) solutions [19]. The dc heating solution can warm low-temperature batteries with a constant-current discharging of the batteries. The current amplitude and duration must be restricted to prevent permanent damage to battery health, thereby leading to a low heating generation rate [20], [21]. By comparison, the ac heating solution can heat batteries by alternately charging and discharging batteries, which avoids substantial change of

Manuscript received February 16, 2018; revised May 14, 2018 and June 10, 2018; accepted July 14, 2018. Date of publication August 9, 2018; date of current version January 31, 2019. This work was supported by Gotion Inc. (*Corresponding author: Chunting Chris Mi.*)

The authors are with the Department of Electrical and Computer Engineering, San Diego State University, San Diego, CA 92182 USA (e-mail: yshang@sdsu.edu; chong.zhu@sdsu.edu; YFU@mail.sdsu.edu; mi@ieee.org).

Color versions of one or more of the figures in this paper are available online at <http://ieeexplore.ieee.org>.

Digital Object Identifier 10.1109/TIE.2018.2863187

the state-of-charge and lithium deposition [22]. Therefore, the ac heating solution is more effective with less effect on battery health than the dc solution [19].

Zhang *et al.* [23] developed an internal low-frequency ac heating method for low-temperature batteries and showed that the ac amplitude and frequency had a significant impact on the heat-generation rate. Moreover, they pointed out that the ac heating method had slightly damaged the batteries. Jiang *et al.* [24] built a thermoelectric model to capture both the electrical and thermal behaviors of batteries at low temperatures. Mohan *et al.* [25] proposed a predictive control-based heating technique, which optimized the magnitude of a sequence of bidirectional currents to minimize the total energy loss. Wang *et al.* [26], [27] reported a new “all-climate” lithium-ion battery structure, which could heat itself up in extremely cold weather. It only took 20 s to heat the battery from -20 to 0 °C, consuming only 3.8% of cell energy. In fact, it belongs to the dc-discharging heating method, which cannot be directly applied to general batteries. Fortunately, Stuart *et al.* [28] designed a high-frequency converter to heat NiMH batteries of hybrid electric vehicles (HEVs) at subzero temperatures. The drawback is that the heater is supplied by the onboard generator driven by the HEV’s heat engine, which cannot be easily applied to EVs.

For battery equalization, there are mainly active and passive balancing methods [10], [13]–[15]. The active balancing methods [10] usually use capacitors, inductors, transformers, or their combinations to transfer energy from cell to cell, cell to pack, or pack to cell. Although these solutions achieve higher balancing efficiency, they have the obvious disadvantage of bulky size, high cost, complex control, and low reliability. By contrast, the passive balancing solution [14] employs a small resistor for each cell to consume excess energy from the more charged cells, which is the only one currently applied to commercial EVs because of the outstanding advantages of compact size, low price, and simple implementation. However, the main disadvantage is the zero balancing efficiency.

It is worth mentioning that Shang *et al.* [13] proposed an integrated heater equalizer based on buck–boost conversion without the need of external power supplies. At lower switching frequencies, the topology can heat up low-temperature batteries. At higher switching frequencies, it can achieve the adjacent cell-to-cell balancing for series-connected battery strings. However, this topology uses a large number of components, leading to complex implementation and degraded reliability. In particular, the plentiful heat in MOSFETs due to the conduction and switching losses is not utilized to externally warm batteries, leading to a long heating time and a low efficiency.

In order to address the preheating issue of the onboard batteries in cold climates and deal with the inconsistency of cell voltages, this paper proposes an integrated heater equalizer for series-connected lithium-ion battery strings of EVs, which has the features of compact size, low cost, high reliability, and ease of implementation. This paper is an extension and improvement of the previous work [15]. There are three original important contributions. First, based on balancing technologies, an onboard heater with internal and external combined heating is proposed without the requirement of external power supplies,

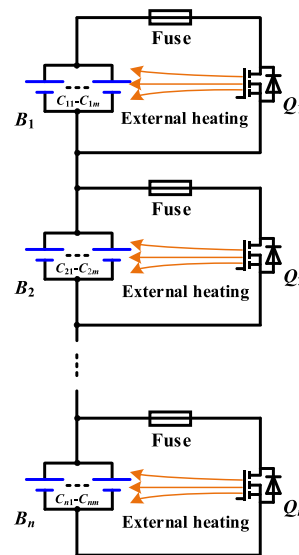


Fig. 1. Proposed integrated heater-equalizer for a practical EV lithium-ion battery string.

achieving a fast heating speed and high efficiency. Second, a thermoelectric model for the internal and external combined heating is developed to accurately predict battery temperature rises at different switching frequencies and duty cycles, which provides insight for the optimization design of the proposed heater. Finally, it is proved that the heating speed and efficiency can be significantly improved by increasing the heating frequency due to the heat generation of battery electrochemical reaction.

II. PROPOSED INTEGRATED HEATER EQUALIZER

A. Topology Configuration

Fig. 1 shows the schematic diagram of the proposed integrated heater equalizer applied to a practical EV lithium-ion battery string, which is usually constituted by thousands of cells first connected in parallel and then connected in series. It can be seen that only one MOSFET and one fuse are needed for the parallel-connected cells, so that the number of the MOSFETs mainly depends on the number of the series-connected cells, leading to a compact size, low cost, and ease of implementation. In addition, the fuses can protect batteries from being over discharged when the MOSFETs fail. It is worth mentioning that in order to achieve the external heating, the MOSFETs should be placed in close proximity to the batteries so that the heat generated in the MOSFETs can be effectively transferred to batteries by air, liquid, or metal as the medium, which significantly improves the heating speed and efficiency.

B. Operation Principles

The proposed heater is driven by a pulsewidth modulation (PWM) signal with adjustable switching frequencies and duty cycles, and has two steady working states during one switching period. Fig. 2(a) and (b) shows the two heating states of the proposed heater for two series-connected battery cells. In

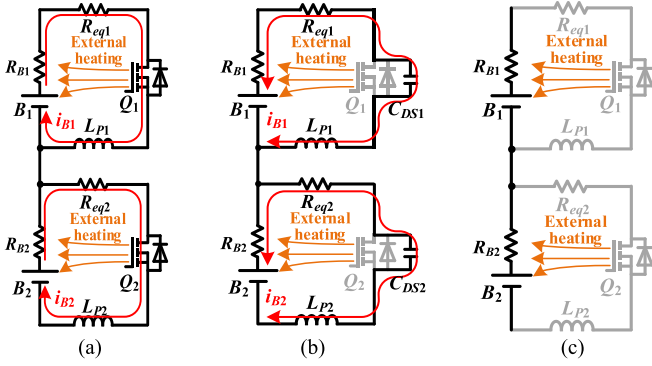


Fig. 2. Operating principles of battery heating for two series-connected battery cells. (a) Heating state I. (b) and (c) Heating state II.

Fig. 2, R_B represents the internal resistance of one battery cell, L_P represents the parasitic inductance in the circuit, C_{DS} represents the drain-source capacitance of the MOSFET, and R_{eq} represents the equivalent resistance in the circuit, which can be given by

$$R_{eq} = R_W + R_I + R_{DS(on)}, \quad (1)$$

where R_W is the wire resistance, R_I is the interconnect resistance, and $R_{DS(on)}$ is the static drain source on the resistance of MOSFET.

Heating State I: As shown in Fig. 2(a), the MOSFETs are turned ON, and the batteries are discharged. Due to the parasitic inductance in the circuit, the discharging current ramps up. Therefore, the discharging current can be regulated by controlling the switching frequency and duty cycle. During this state, the batteries can be internally self-heated by the ohmic and electrochemical losses of batteries, and externally warmed by the heat of the MOSFETs using the switching and conduction losses.

Heating State II: As shown in Fig. 2(b), when the MOSFETs are turned OFF, the energy stored in the parasitic inductance will be quickly released to the drain-source capacitance of the MOSFET, which activates a damped oscillating current. After this transient state, the heating current completely decreases to 0, as shown in Fig. 2(c). It can be seen that during State II, the batteries are mainly warmed externally by the heat of the MOSFETs.

It can be seen that the proposed heater can take full advantage of the energy losses in batteries and MOSFETs to heat low-temperature batteries, significantly improving the heating speed and efficiency. It is worth mentioning that battery heating makes a contribution to balance the cell voltages because the heating currents are proportional to the cell voltages.

The purpose of battery balancing is to ensure that all the cell voltages are equal. Similar to the proposed heating, the battery balancing also has two similar working states, as shown in Fig. 2. However, the biggest difference is that only the parallel-connected MOSFETs of the higher-voltage cells are activated so that the higher cell voltages can be balanced to the lower cell voltage. It is important to note that the inconsistency of a battery string develops very slowly so there is enough time to

balance the imbalanced cells with a small balancing current. In addition, a large balancing current may cause harm to batteries. Therefore, the proposed integrated topology should work at higher switching frequencies and smaller duty cycles to achieve a small discharging current and reduce the negative effect on battery health.

In summary, the proposed battery heating-balancing solution has the following favorable features.

- 1) The proposed topology only needs one MOSFET for each cell, resulting in a compact size and low cost, which can be easily applied to EVs.
- 2) All MOSFETs are driven by one high-frequency PWM signal, so that the batteries can be heated internally by the ohmic and electrochemical losses and warmed externally by the switching and conduction losses of the MOSFETs, leading to a fast heating speed and high efficiency.
- 3) By activating the parallel-connected MOSFETs of the higher-voltage cells at higher switching frequencies and smaller duty cycles, the proposed system can also balance the cell voltages like the passive equalizer [14], dramatically improving the power density.
- 4) Because the discharging current depends on the cell voltage, battery heating has also a positive effect in balancing cell voltages.

III. THERMOELECTRIC MODEL FOR INTERNAL AND EXTERNAL COMBINED HEATING

In order to provide guidance for the optimized design of the proposed heater, a thermoelectric model for the internal and external combined heating is developed to accurately predict the battery temperature rises at different switching frequencies and duty cycles.

As shown in Fig. 2, based on Kirchhoff's current law, the discharge current for one cell during one switching period can be expressed as

$$\begin{cases} i_B(t) = \frac{V_B}{R_{eq}} - \frac{L_p}{R_{eq}} \cdot \frac{di_B}{dt}, & 0 < t \leq DT_{SW} \\ i_B(t) = 0, & DT_{SW} < t \leq T_{SW} \end{cases} \quad (2)$$

where V_B is the cell voltage, L_p is the parasitic inductance, T_{SW} is the switching period, and D is the duty cycle.

With $i_B(0) = 0$, (2) can be solved as

$$\begin{cases} i_B(t) = \frac{V_B}{R_{eq}} \left(1 - e^{-\frac{R_{eq}}{L_p} t} \right), & 0 < t \leq DT_{SW} \\ i_B(t) = 0, & DT_{SW} < t \leq T_{SW} \end{cases} \quad (3)$$

As t approaches zero at higher switching frequencies, (3) can be approximately represented by

$$\begin{cases} i_B(t) \approx \frac{V_B}{L_p} t, & 0 < t \leq DT_{SW} \\ i_B(t) = 0, & DT_{SW} < t \leq T_{SW} \end{cases} \quad (4)$$

It can be seen that at higher switching frequencies, the impedance of the proposed heater is mainly dependent on the

parasitic inductance, neglecting the small switch, wire, and interconnect resistances.

According to (4), the rms value can be approximately derived

$$I_{B(\text{RMS})} \approx \frac{V_B D^2}{2fL_P} \quad (5)$$

where f is the switching frequency, which is equal to $1/T_{\text{SW}}$. Equation (5) shows that the rms heating current can be regulated by controlling the switching frequency f and duty cycle D .

Model 18650 battery cells have almost the same internal and surface temperatures [17], [23], [24]. Thus, the thermoelectric model of the internal heating can be described by

$$mc \frac{dT}{dt} + hS(T - T_0) = I_{B(\text{RMS})}^2 R_B + fQ_E \quad (6)$$

where T is the battery temperature, T_0 is the ambient temperature, m is the battery mass, c is the specific heat capacity, S is the surface area of the battery, h is the equivalent heat transfer coefficient, and Q_E represents the heat generated by battery electrochemical reaction during one switching period. Experimental results show that Q_E is basically proportional to the rms heating current I_{rms} and is independent of the switching frequency f [17], [23], [24]. fQ_E shows that the electrochemical reaction will generate more heat at a higher switching frequency.

With the same battery temperature and rms heating current, by calculating (6) at lower and higher switching frequencies, the electrochemical heat Q_E during one switching period can be derived

$$Q_E = \frac{mc \left(\frac{dT_h}{dt} - \frac{dT_l}{dt} \right)}{f_h - f_l} \quad (7)$$

where f_l and f_h represent the lower and higher switching frequencies, respectively. T_l and T_h represent the battery temperature rises at the lower and higher switching frequencies, respectively.

Further, the thermoelectric model for the internal and external combined heating can be described by

$$mc \frac{dT}{dt} + hS(T - T_0) = I_{B(\text{RMS})}^2 R_B + fQ_E + \lambda \left\{ I_{B(\text{RMS})}^2 R_{\text{DS(on)}} + \frac{1}{2} f C_{\text{DS}} V_B^2 + \frac{1}{2} f V_B I_{B(\text{RMS})} t_f \right\} \quad (8)$$

where the third term in (8) represents the external heating from MOSFETs. Considering that the heat generated in MOSFETs cannot be totally delivered to batteries, a coefficient of heat conduction λ is introduced, which is between 0 and 1. $I_{B(\text{RMS})}^2 R_{\text{DS(on)}}$ represents the conduction loss, $\frac{1}{2} f C_{\text{DS}} V_B^2$ represents the turn-ON switching loss, C_{DS} represents the drain-source capacitance of MOSFETs, $\frac{1}{2} f V_B I_{B(\text{RMS})} t_f$ represents the turn-OFF switching loss, t_f is the fall time of MOSFETs, and $hS(T - T_0)$ represents the heat diffusion to the environment.

With the same battery temperature, rms heating current, and switching frequency, by subtracting (6) from (8), the heat

conduction coefficient λ can be derived

$$\lambda = \frac{mc \left(\frac{dT_c}{dt} - \frac{dT_l}{dt} \right)}{I_{B(\text{RMS})}^2 R_{\text{DS(on)}} + \frac{1}{2} f C_{\text{DS}} V_B^2 + \frac{1}{2} f V_B I_{B(\text{RMS})} t_f} \quad (9)$$

where T_c and T_l represent the battery temperature rises with the internal–external combined heating and the internal heating, respectively.

Combining (5) and (8), the thermoelectric model of the internal–external combined heating can be further expressed as

$$mc \frac{dT}{dt} + hS(T - T_0) = \frac{V_B^2}{2} \left\{ \frac{D^4}{2f^2 L_P^2} R_B + \lambda \left(\frac{D^4}{2f^2 L_P^2} R_{\text{DS(on)}} + f C_{\text{DS}} + \frac{D^2}{2L_P} t_f \right) \right\} + fQ_E. \quad (10)$$

By solving (10), the battery temperature rise T can be derived

$$T = \left(T_0 - \frac{hST_0 + A}{hS} \right) e^{-\frac{hS}{mc}t} + \frac{hST_0 + A}{hS} \quad (11)$$

where

$$A = \frac{V_B^2}{2} \left\{ \frac{D^4}{2f^2 L_P^2} R_B + \lambda \left(\frac{D^4}{2f^2 L_P^2} R_{\text{DS(on)}} + f C_{\text{DS}} + \frac{D^2}{2L_P} t_f \right) \right\} + fQ_E. \quad (12)$$

It can be seen from (8) to (12) that the ohmic loss of batteries and the conduction loss of MOSFETs can be increased by decreasing the switching frequency or increasing the duty cycle due to the increase in the rms heating current. On the contrary, the electrochemical heat and the switching loss can be increased by increasing the switching frequency. Therefore, with the same rms heating current, i.e., the same damage to batteries, a higher switching frequency is preferred to achieve a faster heating speed and less heat diffusion to the environment.

It is important to note that a larger internal resistance of batteries R_B and a smaller drain source on resistance $R_{\text{DS(on)}}$ will lead to a higher internal heating efficiency, which means more energy used for internally heating batteries. However, the external heating depends mainly on the switching and conduction losses of MOSFETs, which needs a larger $R_{\text{DS(on)}}$. Therefore, $R_{\text{DS(on)}}$ should be carefully selected to achieve the tradeoff between the internal and external heating effects.

IV. EXPERIMENTAL RESULTS

As shown in Fig. 3(a), a prototype for two 2500-mAh LiNiMnCoO₂ cells is built. Switches Q_1 and Q_2 are implemented by IRFZ30 MOSFETs. Table I presents the parameters used for calculation of the thermoelectric model [23], [29]. The cell temperatures were measured by thermistors and the measurement points are shown in Fig. 3(a). The two-dimensional cell temperature distributions were measured by the infrared thermometer Fluke Ti125. In order to quickly cool down the batteries to the setting temperature, e.g., -20 °C, the ambient temperature was first set at a lower temperature, e.g., -25 °C.

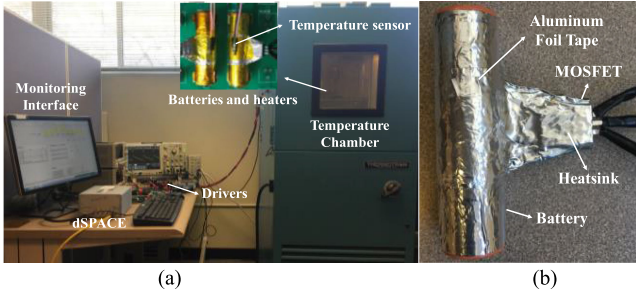


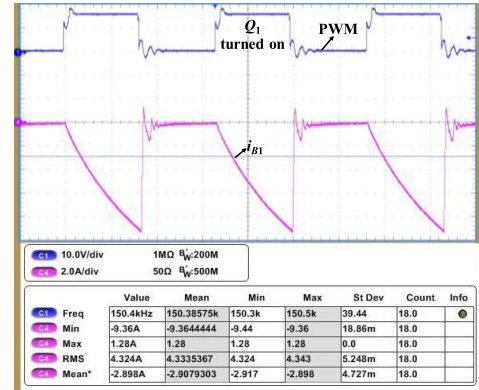
Fig. 3. Experiment setup. (a) Test platform. (b) Implementation of the external heating from a MOSFET to a battery.

TABLE I
PARAMETERS USED IN CALCULATION OF THE THERMOELECTRIC MODEL [23], [29]

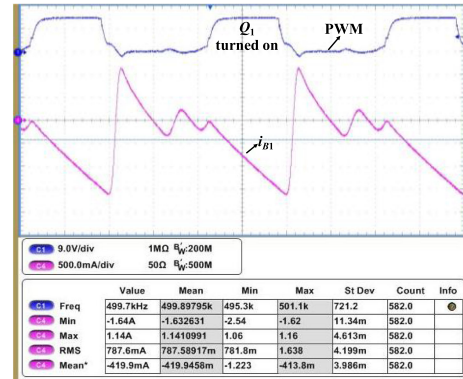
Parameter	Symbol	Value
Battery mass	m	46.0 g
Battery surface area	S	$4.18 \times 10^{-3} \text{ m}^2$
Specific heat capacity	c	$1.72 \text{ J g}^{-1} \text{ K}^{-1}$
Equivalent heat transfer coefficient	h	$15.9 \text{ W m}^{-2} \text{ K}^{-1}$
Battery internal resistance at -20°C	R_B	394 m Ω
Parasitic inductance	L_p	0.95 μH
Drain-source on resistance of MOSFETs	$R_{DS(on)}$	50 m Ω
Drain-source capacitance of MOSFETs	C_{DS}	800 pF
Fall time of MOSFETs	t_f	35 ns

When the cell temperatures reached -20°C for 1 h, the ambient temperature was set to -20°C for 2 h before heating. Fig. 3(b) shows one implementation method of the external heating for batteries. A battery and the heatsink of a MOSFET are wrapped and connected by the aluminum foil tapes so that the heat generated in the MOSFET can be effectively conducted to the outside of the battery, by which the external heating is achieved. It is important to note that battery balancing has little effect on the battery temperature rise due to the smaller balancing current, which causes less heat in the batteries and MOSFETs.

Fig. 4 shows the experimental waveforms of the proposed system for heating and balancing batteries, respectively. As shown in Fig. 4(a), when the switching frequency is set to $f = 150 \text{ kHz}$ and the duty cycle is set to $D = 50\%$, the heating current is a ramp wave due to the influence of the parasitic inductance in the circuit. The amplitude of the discharge current is 9.36 A, i.e., 3.7 C , and the rms value is 4.32 A, i.e., 1.7 C . As shown in Fig. 4(b), when the switching frequency increases to $f = 500 \text{ kHz}$ and the duty cycle decreases to $D = 40\%$, the amplitude of the discharge current is reduced to 1.64 A with the mean value of 419.9 mA, which is fit for balancing cell voltages. It is important to note that when the MOSFET is turned OFF, a damped oscillating current is activated because the parasitic inductance and the drain-source capacitance of the MOSFET form an LC resonant circuit. These results show that the proposed scheme can heat batteries at low temperatures with a lower switching frequency and larger duty cycle and balance cell voltages with a higher switching frequency and smaller duty cycle.



(a)



(b)

Fig. 4. Experimental waveforms of the proposed topology. (a) At $f = 150 \text{ kHz}$ and $D = 50\%$. (b) At $f = 500 \text{ kHz}$ and $D = 40\%$.

Fig. 5(a) shows the internal resistances of the LiNiMnCoO₂ battery at different cell temperatures. It can be seen that the lower the cell temperature, the larger the cell resistance. The internal resistance decreases from 349 to 218 m Ω as the cell temperature increases from -20 to 0°C . Fig. 5(b) further presents the measured rms heating current at different cell temperatures under $f = 150 \text{ kHz}$ and $D = 50\%$. Due to the decrease in the battery internal resistance, the rms heating current increases from 4.32 A at -20°C to 4.65 A at 0°C . Therefore, according to (6), the internal heating effect is hardly affected by the cell temperature because of the decrease in the internal resistance and the increase in the rms current. It is important to note that the decrease in the battery internal resistance leads to a small increase, i.e., 0.33 A, in the rms heating current, which would not cause damage to the battery.

Fig. 6(a) shows the comparative internal heating results for two LiNiMnCoO₂ cells at different switching frequencies with almost the same rms heating current of 3 A, i.e., 1.2 C . It can be seen that at $f = 50 \text{ kHz}$, it takes 13.2 min to heat batteries from -20 to 0°C and the average temperature rise rate is only $1.5^\circ \text{C}/\text{min}$. By comparison, when the switching frequency is increased to 150 kHz , the heating time is reduced to 4.3 min and the temperature rise rate reaches $6.7^\circ \text{C}/\text{min}$ because of the larger electrochemical heat fQ_E at the higher switching frequency. Based on (7), the electrochemical heat Q_E during one switching period is calculated as $4.27 \times 10^{-5} \text{ J}$. Overall, the calculated

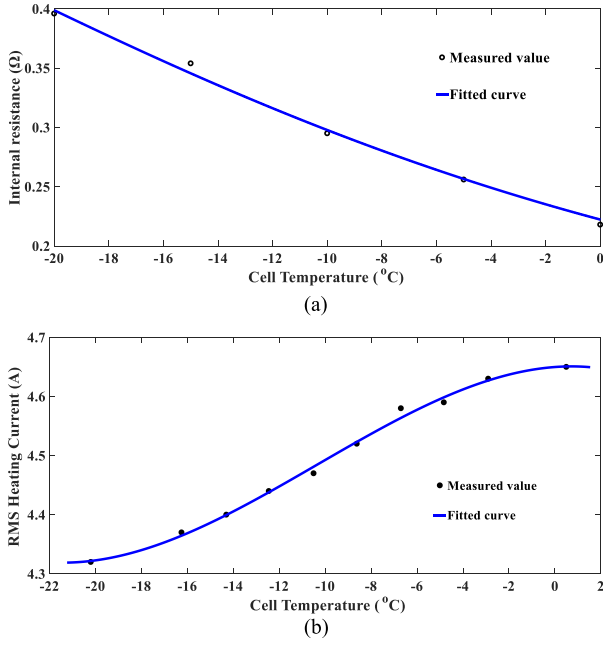


Fig. 5. (a) Measured battery internal resistance versus cell temperature. (b) Measured rms heating current versus cell temperature.

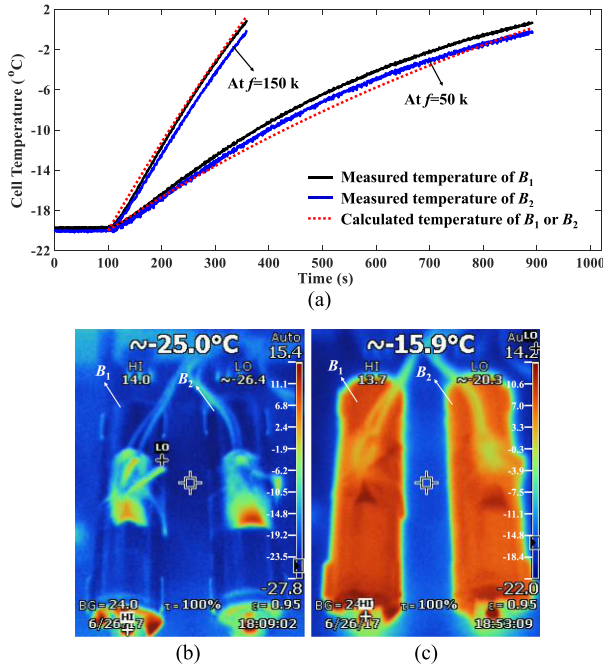


Fig. 6. Comparative internal-heating results for two LiNiMnCoO₂ cells at different switching frequencies with the same rms heating current. (a) Temperature rises. (b) and (c) Cell heat distributions before and after heating.

cell temperature curves fit well with the measured values at the switching frequencies of 50 and 150 kHz, respectively, which proved the validity of (6). Fig. 6(b) and (c) further shows the cell temperature distributions before and after heating, which proved the good heating consistency.

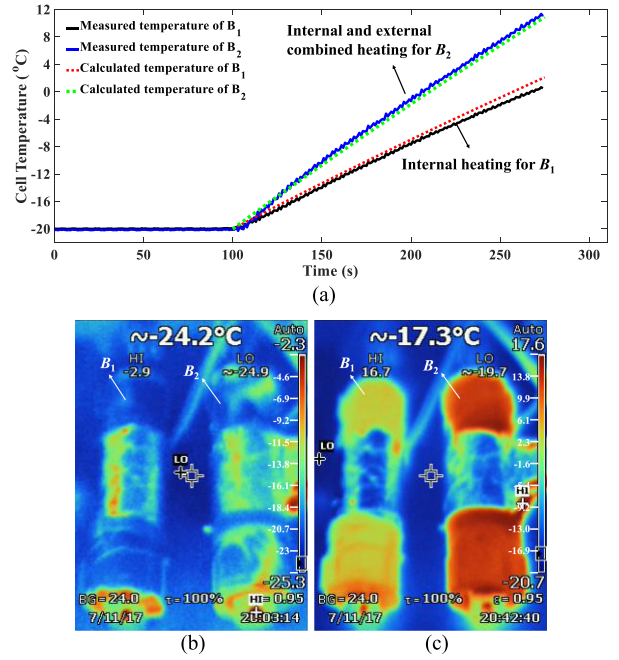


Fig. 7. Comparative heating results for two LiNiMnCoO₂ cells with internal heating and internal-external combined heating at the ambient temperature of -20 °C. (a) Temperature rises. (b) and (c) Cell heat distributions before and after heating.

TABLE II
COMPARISON OF THE HEATING RESULTS WITH THE INTERNAL HEATING AND THE INTERNAL-EXTERNAL COMBINED HEATING

Heating method	Heating time ^①	Temperature rise rate	Battery loss	MOSFET loss ^②
Internal heating	2.9 mins	6.9 °C/min	6.5%	2.1%
Internal-external heating	1.9 mins	10.5 °C/min	5.0%	1.6%

① The heating time is represented by the total time to heat batteries from -20 to 0 °C.
② Because the energy consumed by the MOSFET comes from the battery, the MOSFET loss is represented by its proportion of the total battery energy.

In order to verify the validity of the external heating, Fig. 7 shows the comparative heating results with the internal heating and the internal-external combined heating at the ambient temperature of -20 °C. The switching frequency is set as $f = 150$ kHz and the duty cycle is set as $D = 50\%$. The average rms current is about 4.32 A, i.e., 1.7 C. B₁ is only heated internally, while B₂ is internally and externally heated. Based on (9), the heat conduction coefficient λ is calculated as 0.82. Table II presents the comparative heating results for B₁ and B₂. Because the heat of the MOSFET is effectively utilized to externally warm cell B₂, the average temperature-rise rate of B₂ reaches 10.5 °C/min, which is significantly higher than that of B₁ with the internal heating only, i.e., 6.9 °C/min. Moreover, B₂ only burns about 5% cell energy compared to 6.5% energy loss of B₁. Therefore, about 1.5% cell energy is saved by the external heating. According to $\lambda = 0.82$ and 1.6% MOSFET loss, about 1.3% cell energy is recycled to externally heat the battery, increasing the heating speed and efficiency. Overall, the calculated cell temperature curves agree with the measured

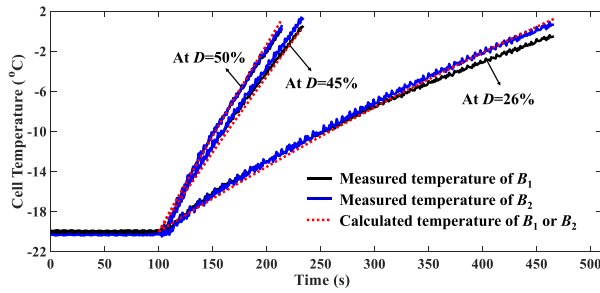


Fig. 8. Internal-external combined heating results for two LiNiMnCoO₂ cells with different duty cycles under the switching frequency of $f = 150$ kHz at the ambient temperature of -20 °C.

TABLE III

COMPARISON OF THE HEATING RESULTS WITH DIFFERENT DUTY CYCLES

Duty cycle	RMS current	Heating time	Temperature rise rate	Electrochemical heat Q_E
26%	2.3 A	6.1 min	3.3 °C/min	3.27×10^{-5} J
45%	4.2 A	2.2 min	9.1 °C/min	5.98×10^{-5} J
50%	4.5 A	1.9 min	10.5 °C/min	6.41×10^{-5} J

TABLE IV

CAPACITIES OF BATTERIES VERSUS HEATING CYCLES

Heating cycle	Cell B ₁		Cell B ₂	
	Capacity	Capacity loss	Capacity	Capacity loss
0	2.27 Ah	0%	2.28 Ah	0%
30	2.27 Ah	0%	2.26 Ah	0.9%
100	2.21 Ah	3%	2.21 Ah	3.1%

ones under the internal heating and internal-external combined heating, respectively, which proved the validity of (6) and (8). Fig. 7(c) further shows the different temperature distributions of the two cells after heating compared with the consistent initial temperature distribution shown in Fig. 7(b). In summary, these results effectively verified the validity of the external heating.

Fig. 8 shows the comparative heating results with different duty cycles under the switching frequency of $f = 150$ kHz at the ambient temperature of -20 °C. Table III presents a comparison of the heating results. It can be observed that the heating speed can be significantly improved by increasing the duty cycle D due to the increasing rms current. It is important to note that by comparing the electrochemical heats with the rms currents at different duty cycles, it is proved that the electrochemical heat Q_E is basically proportional to the rms heating current I_{rms} .

In order to analyze the influence of the heating on battery health, Table IV presents the cell capacities versus heating cycles. It can be observed that there is hardly any decrease in capacities of the two cells after 30 heating cycles. Nevertheless, about 3% cell capacity fade is achieved at the end of 100 heating cycles. It is assumed that one year has 30 days with extreme weather below -20 °C, based on which 100 heating cycles would guarantee the battery operating for about 3.3 years.

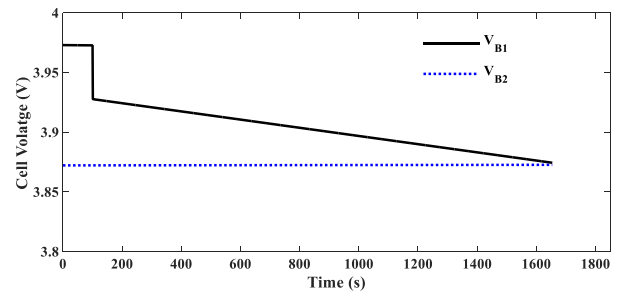


Fig. 9. Balancing result for two LiNiMnCoO₂ cells under $f = 500$ kHz and $D = 40\%$ at room temperature.

Therefore, the battery life is not noticeably affected by the proposed battery heating in extreme weather.

Fig. 9 shows the passive balancing result of the proposed system for two LiNiMnCoO₂ cells at room temperature. Since $V_{B1} > V_{B2}$, B₁ is periodically discharged by the parallel-connected MOSFET, which is driven by a PWM signal with $f = 500$ kHz and $D = 40\%$. It can be seen that after 1554-s discharge balancing, the higher cell voltage V_{B1} decreases to the lower cell voltage V_{B2} , and the balancing among the two cells is achieved. This proved that the proposed heater can also balance the cell voltages at a higher switching frequency and smaller duty cycle.

V. CONCLUSION

The purpose of this paper was to introduce an automotive onboard heater equalizer to internally and externally preheat cold lithium-ion batteries and balance cell voltages without requiring additional devices. The design procedure was presented, the thermoelectric model for the internal and external combined heating was developed, and a prototype for two LiNiMnCoO₂ cells was built.

Experimental results demonstrated the following.

- 1) The proposed topology can effectively heat low-temperature lithium-ion batteries with a fast speed, high efficiency, and good consistency.
- 2) With the same rms heating current, the heating speed can be significantly improved by increasing the switching frequency.
- 3) The heat generated in the MOSFETs can externally warm batteries as an effective complementarity of the internal heating.
- 4) The proposed internal and external combined heater has little damage to batteries.
- 5) The proposed topology can also balance cell voltages with the same control at a higher frequency and lower duty cycle without the requirement of additional balancing circuits, significantly increasing the power density of battery management systems.

In the future, an adaptive control algorithm will be introduced to adjust the switching frequency during heating so that the batteries can be heated with a good tradeoff between heating speed and the impact on battery health.

REFERENCES

- [1] H. Rahimi-Eichi, U. Ojha, F. Baronti, and M. Chow, "Battery management system: An overview of its application in the smart grid and electric vehicles," *IEEE Ind. Electron. Mag.*, vol. 7, no. 2, pp. 4–16, Jun. 2013.
- [2] C. Zhang, K. Li, J. Deng, and S. Song, "Improved realtime state-of-charge estimation of LiFePO₄ battery based on a novel thermoelectric model," *IEEE Trans. Ind. Electron.*, vol. 64, no. 1, pp. 654–663, Jan. 2017.
- [3] Y. Ji, Y. Zhang, and C.-Y. Wang, "Li-ion cell operation at low temperatures," *J. Electrochem. Soc.*, vol. 160, no. 4, pp. 636–649, Feb. 2013.
- [4] M. Armand and J.-M. Tarascon, "Building better batteries," *Nature*, vol. 451, no. 7179, pp. 652–657, Feb. 2008.
- [5] W. Huang and J. Qahouq, "An online battery impedance measurement method using dc-dc power converter control," *IEEE Trans. Ind. Electron.*, vol. 61, no. 11, pp. 5987–5995, Nov. 2014.
- [6] *Extreme temperatures affect electric vehicle driving range*. Mar. 2014. [Online]. Available: <http://newsroom.aaa.com/2014/03/extreme-temperatures-affect-electric-vehicle-driving-range-aaa-says/>. Accessed on: Feb 9, 2018.
- [7] S. Zhang, K. Xu, and T. Jow, "The low temperature performance of Li-ion batteries," *J. Power Sources*, vol. 115, no. 1, pp. 137–140, Mar. 2003.
- [8] S. S. Zhang, K. Xu, and T. R. Jow, "Electrochemical impedance study on the low temperature of Li-ion batteries," *Electrochim. Acta*, vol. 49, no. 7, pp. 1057–1061, Mar. 2004.
- [9] L. Liao *et al.*, "Effects of temperature on charge/discharge behaviors of LiFePO₄ cathode for Li-ion batteries," *Electrochim. Acta*, vol. 60, pp. 269–273, Jan. 2012.
- [10] Y. Shang, C. Zhang, N. Cui, and J. M. Guerrero, "A cell-to-cell battery equalizer with zero-current switching and zero-voltage gap based on quasi-resonant LC converter and boost converter," *IEEE Trans. Power Electron.*, vol. 30, no. 7, pp. 3731–3747, Jul. 2015.
- [11] N. H. Kutkut, "Life cycle testing of series battery strings with individual battery equalizers," Accessed on: Feb 13, 2018. [Online]. Available: <http://citeseerx.ist.psu.edu/viewdoc/summary?doi=10.1.1.497.1611>.
- [12] *Tear down of 85 kWh Tesla battery pack shows it could actually only be a 81 kWh pack*. Feb. 2014. [Online]. Available: <https://electrek.co/2016/02/03/tesla-battery-tear-85-kwh/>. Accessed on: Feb. 9, 2018.
- [13] Y. Shang, B. Xia, N. Cui, C. Zhang, and C. Mi, "An automotive onboard AC heater without external power supplies for lithium-ion batteries at low temperatures," *IEEE Trans. Power Electron.*, vol. 33, no. 9, pp. 7759–7769, Sep. 2018.
- [14] J. Gallardo-Lozano, E. Romero-Cadaval, M. I. Milanés-Montero, and M. A. Guerrero-Martinez, "A novel active battery equalization control with on-line unhealthy cell detection and cell change decision," *J. Power Sources*, vol. 299, pp. 356–370, 2015.
- [15] Y. Shang, C. Zhang, N. Cui, and C. Mi, "A fast-speed heater with internal and external heating for lithium-ion batteries at low temperatures," in *Proc. IEEE Appl. Power Electron. Conf.*, 2018, pp. 3440–3443.
- [16] A.-A. Pesaran, "Battery thermal management in EVs and HEVs: Issues and solutions," in *Proc. Adv. Automotive Battery Conf.*, 2001, pp. 1–10.
- [17] H. Ruan *et al.*, "A rapid low-temperature internal heating strategy with optimal frequency based on constant polarization voltage for lithium-ion batteries," *Appl. Energy*, vol. 177, pp. 771–782, Sep. 2016.
- [18] A.-A. Pesaran, A. Vlahinos, and T. Stuart, "Cooling and preheating of batteries in hybrid electric vehicles," in *Proc. 6th ASME-JSME Therm. Eng. Joint Conf.*, 2003, pp. 1–7.
- [19] Y. Ji and C. Y. Wang, "Heating strategies for Li-ion batteries operated from subzero temperatures," *Electrochim. Acta*, vol. 107, pp. 664–674, Sep. 2013.
- [20] J. Jiang, Q. Liu, C. Zhang, and W. Zhang, "Evaluation of acceptable charging current of power Li-ion batteries based on polarization characteristics," *IEEE Trans. Ind. Electron.*, vol. 61, no. 12, pp. 6844–6851, Dec. 2014.
- [21] L.-R. Chen, J.-J. Chen, C.-M. Ho, S.-L. Wu, and D.-T. Shieh, "Improvement of Li-ion battery discharging performance by pulse and sinusoidal current strategies," *IEEE Trans. Ind. Electron.*, vol. 60, no. 12, pp. 5620–5628, Dec. 2013.
- [22] F. Savoye, P. Venet, M. Millet, and J. Groot, "Impact of periodic current pulses on Li-ion battery performance," *IEEE Trans. Ind. Electron.*, vol. 59, no. 9, pp. 3481–3488, Sep. 2012.
- [23] J. Zhang, H. Ge, Z. Li, and Z. Ding, "Internal heating of lithium-ion batteries using alternating current based on the heat generation model in frequency domain," *J. Power Sources*, vol. 273, pp. 1030–1037, Jan. 2015.
- [24] J. Jiang *et al.*, "A reduced low-temperature electro-thermal coupled model for lithium-ion batteries," *Appl. Energy*, vol. 177, pp. 804–816, Sep. 2016.
- [25] S. Mohan, Y. Kim, and A. G. Stefanopoulou, "Energy-conscious warm-up of li-ion cells from subzero temperatures," *IEEE Trans. Ind. Electron.*, vol. 63, no. 5, pp. 2954–2964, May 2016.
- [26] C. Wang *et al.*, "Lithium-ion battery structure that self-heats at low temperatures," *Nature*, vol. 529, no. 7587, pp. 515–518, Jan. 2016.
- [27] G. Zhang, S. Ge, T. Xu, X.-G. Yang, H. Tian, and C.-Y. Wang, "Rapid self-heating and internal temperature sensing of lithium-ion batteries at low temperatures," *Electrochim. Acta*, vol. 218, pp. 149–155, Nov. 2016.
- [28] T. A. Stuart and A. Hande, "HEV battery heating using AC currents," *J. Power Sources*, vol. 129, pp. 368–378, Apr. 2004.
- [29] International Rectifier, "Hexfet transistor N-channel 50 volt power MOS-FETs," *IRFZ30 datasheet*, Apr. 1987. [Online]. Available: <https://media.digikey.com/pdf/Data%20Sheets/International%20Rectifier%20PDFs/IRFZ30,%20IRFZ32.pdf>



Yunlong Shang (S'14–M'18) received the B.S. degree in automation from the Hefei University of Technology, Hefei, China, in 2008, and the Ph.D. degree in control theory and control engineering from Shandong University, Shandong, China, in 2017.

Between September 2015 and October 2017, he was involved in a scientific research as a joint Ph.D. student with the DOE GATE Center for Electric Drive Transportation, San Diego State University, San Diego, CA, USA. Since 2017, he has been a Postdoctoral Research Fellow with San Diego State University. His research interests include battery equalizers, battery modeling, battery states estimation, and battery management systems of electric vehicles.



Chong Zhu (M'17) received the B.S. degree in electrical engineering from the China University of Mining and Technology, Xuzhou, China, in 2006 and the Ph.D. degree in electrical engineering from Zhejiang University, Hangzhou, China, in 2016.

He is currently a Postdoctoral Researcher with San Diego State University, San Diego, California, CA, USA. His research interests include battery thermal management, ac-dc power conversion, and PWM techniques applied in EVs.



Yuhong Fu received the M.S. degree in automotive systems engineering from the University of Michigan-Dearborn, Dearborn, MI, USA, in December 2011.

She is currently with San Diego State University, San Diego, CA, USA. Her research interests include battery modeling and management for electric drive vehicle applications.



Chunting Chris Mi (S'00–A'01–M'01–SM'03–F'12) received the B.S.E.E. and M.S.E.E. degrees in electrical engineering from Northwestern Polytechnical University, Xi'an, China, in 1985 and 1988, respectively, and the Ph.D. degree in electrical engineering from the University of Toronto, Toronto, ON, Canada in 2001.

He is a Professor and Chair of electrical and computer engineering and the Director of the Department of Energy (DOE) funded Graduate Automotive Technology Education (GATE) Center for Electric Drive Transportation, San Diego State University, San Diego, CA, USA. From 2001 to 2015, he was with the University of Michigan, Dearborn, MI, USA. His research interests include electric drives, power electronics, electric machines, renewable-energy systems, and electric and hybrid vehicles.